Commandeering a biological pathway using aptamer-derived molecular adaptors

Prabhat K. Mallik, Kimi Nishikawa, Albert J. T. Millis and Hua Shi*

Department of Biological Sciences and Institute for RNA Science and Technology, University at Albany, State University of New York, Albany, NY 12222, USA

ABSTRACT

Induction of molecular proximity can mediate a discrete functional response in biological systems. Therefore, creating new and specific connectivity between non-interacting proteins is a means of imposing rational control over biological processes. According to this principle, here we use composite RNA aptamers to generate molecular adaptors that link various 'target' molecules to a common 'utility' molecule, with the utility molecule being an entry point to a pathway conscripted to process the target molecule. In particular, we created a bi-functional aptamer that simultaneously binds to the green fluorescent protein (serving as a surrogate extracellular target) and the opsonin C3b/iC3b (serving as the utility molecule). This bi-functional aptamer enabled us to commandeer the C3-based opsonization-phagocytosis pathway to selectively transport an extracellular target into the lysosome for degradation. This novel strategy has the potential for powerful therapeutic applications with extracellular proteins involved in tumor development or surface markers on cancer cells as the target molecules.

INTRODUCTION

Opsonization is an important immunological mechanism of host defense, in which foreign substances are tagged by opsonin molecules for destruction. The most important opsonins are antibodies and complement proteins such as C3b and its closely related fragment iC3b. These proteins act as adaptors to connect a wide variety of target particles with a few common receptors on effector cells such as macrophages or natural killer (NK) cells. A major consequence of opsonization is phagocytosis, the internalization of particles by phagocytes, which is initiated by the receptor–opsonin interaction (1).

Compared to antibodies, however, C3b/iC3b is less specific and has less capacity as an adaptor. The major reason for this lies in the linkage of C3b/iC3b with the particles it tags. Antibodies interact with their antigens by means of non-covalent binding based on molecular shape and charge distribution; in contrast, C3b/iC3b uses a thioester as its 'warhead' for covalent attachment to the particle being opsonized (2–5). Although C3b shows a preference for certain hydroxyl groups, it has no intrinsic ability to discriminate between self and non-self, and only 10% of activated C3b molecules become linked to antigenic surfaces (6). This feature suggested the possibility of intentionally re-directing C3-based opsonization to destroy disease-causing molecules or cells, especially those that are not recognized by the immune system as 'foreign'. We explored this possibility by equipping C3b/iC3b with an *additional* adaptor that provides higher specificity and efficiency for the purpose of eliciting a response against a predetermined non-natural target.

We envisioned this synthetic adaptor as a composite bi-functional aptamer comprising at least two individual aptamers, one for a target molecule and one for C3b/iC3b. In this configuration, the C3b/iC3b molecule and the aptameric adaptor *together* would function with specificity and efficiency at a similar level to that of antibodies. Aptamers are isolated *in vitro* from a combinatorial sequence pool, with specificity in target recognition rivaling or exceeding the paratopes of antibodies (7,8). Many aptamers can interfere with protein function and some have been used in immunotherapies (9). Our approach would augment the potency of target-binding aptamers so that the targets are not merely neutralized reversibly, but instead destroyed or damaged irreversibly. Here we present data demonstrating the use of such a bi-functional aptamer to mediate specific and efficient transportation of extracellular green fluorescent protein (GFP) into the lysosomes of phagocytic cells for degradation. The general strategies and principles developed in this study are applicable to other systems. In particular, one-time optimization of the interaction between an aptamer and a utility molecule, such as the opsonin

*To whom correspondence should be addressed. Tel: +1 518 591 8840; Fax: +1 518 442 4767; Email: hshi@albany.edu

C3b/iC3b, can be used to construct molecular adaptors targeting many other molecules in conjunction with aptamers developed for those other molecules. Aptamer-mediated opsonization may cause clearance of secreted protein targets by phagocytes, and increased deposition of C3b/iC3b on the surface of the target-bearing cells via aptamer binding may facilitate cytotoxicity by phagocytes and NK cells.

MATERIALS AND METHODS

Proteins and nucleic acids

Human C3 and iC3b proteins were purchased from Calbiochem. Human C3b protein was from Quidel. GFP was purchased from Millipore. Azami Green, mCherry, d2EGFP and the GFP-mCherry fusion protein were gifts from Dr B. Shui and Dr M. Kotlikoff (Cornell University). Oligonucleotides were provided by IDT. RNA aptamers were prepared by *in vitro* transcription using the MAXIscript or MEGAshortscript T7 kit from Ambion. Sequences of aptamers are given below.

AptC3-1:
5′GGGAGAAUUCAACUGCCAUCUAGGCUAGAA GAAUAUGACGGAUUGACCGUAUCAGGGUAGC CGAAGGGAGACAGAAGUACUACAAGCUUCUG GACUCGGU3′.

Apt[C3-GFP]:
5′GGGAGCCUGAUGGCAGGGCGAAUUGGGUGG GGAAAGUCCUUAAAAGAGGGCCACCACAGAA GCAAUGGGCUUCUGGACUCGGUCCCGCUCGG CUAGAAGAAUAUGACGGAUUGACCGUAUCAG GGUAGCCGAGC3′.

AptC3-2:
5′GGGAGAAUUCAACUGCCAUCUAGGCAAAUC CGCGAGCGCCGGUACCGGUGGCGCAUGCCCAC ACAGCACUAAACGAGUACUACAAGCUUCUGG ACUCGGU3′.

Aptamer isolation and characterization

Aptamers for C3 were isolated using protocols described previously (10,11). Binding assays were performed in 20-μl volumes in 1× binding buffer. ^{32}P-labeled RNA probes were prepared using [α-^{32}P]CTP (GE Healthcare). A typical binding mixture with labeled RNA contained ~20 fmol of RNA probe and different amounts (usually 1–10 pmol) of protein. The binding buffer contained 20 mM Tris–HCl (pH 7.6), 150 mM NaCl and 10 mM MgCl$_2$.

The affinity of aptamers to C3, C3b, or iC3b was investigated by electrophoretic mobility shift assay (EMSA) using 6% polyacrylamide gels (acrylamide:*bis*-acrylamide, 70:1). The running buffer contained 10% glycerol, 12.5 mM Tris base, 100 mM glycine and 2.5 mM MgCl$_2$. Binding of the bi-functional aptamer Apt[C3-GFP] to C3, GFP and their derivatives was determined using filter-binding assays with nitrocellulose filters (Millipore) and a Bio-Dot SF (slot format) Microfiltration System (Bio-Rad).

To detect triple complex formation, 10 μg of C3 protein in 50 μl of binding buffer (containing 50 μg/ml of PMSF and 1 μg/ml of aprotinin) was immobilized on a 1 cm^2 nitrocellulose filter presoaked with binding buffer. The filter was blocked with 10 mg/ml bovine serum albumin (BSA) for at least 1 h, and washed with binding buffer. Ten micrograms of bi-functional aptamer (~4-fold the molar quantity of C3) was reconstituted in 100 μl of binding buffer with 40 U of SUPERase•In (Ambion) and incubated on the filter for at least 1 h at 37°C. A comparable amount of yeast total RNA (Ambion) was used as a control. The filter was washed and incubated with 5 μg of GFP in 100 μl of binding buffer, and washed again. Proteins were eluted with 150 μl of elution buffer (20 mM Tris–HCl pH 7.6, 750 mM NaCl), precipitated with trichloroacetic acid, and run on 6–12% SDS–polyacrylamide gradient gels. Western blotting was performed with rabbit anti-GFP antibody (Sigma) and the ECL kit (GE Healthcare).

Cell culture and cell-based assays

THP-1 cells (ATCC) were maintained in RPMI-1640 medium with 10% fetal bovine serum (FBS), 100 U/ml of penicillin, 100 μg/ml of streptomycin and 0.05 mM 2-mercaptoethanol. For immunohistochemistry, cells were induced to differentiate with 50 ng/ml phorbol 12-myristate 13-acetate (PMA) (12,13). Each experiment was repeated at least three times.

For the GFP internalization assays, 1 μg (~10^{13} molecules) of Apt[C3-GFP] was reconstituted in 20 μl of binding buffer (see above), heated at 70°C for 5 min and renatured at 37°C with 40 U of SUPERase•In. The aptamer was mixed with ~6 × 10^{13} molecules (20 μg) of purified iC3b, followed by ~10^{14} molecules (10 μg) of GFP or its derivatives in 200 μl of serum-free RPMI-1640 with 0.1 mg/ml of BSA and 2.5 mM MgCl$_2$ and incubated for 30 min. An additional 300 μl of RPMI-1640 was added. Approximately 2 × 10^6 THP-1 cells were mixed with the prepared complex, and incubated for 15–30 min. Subsequently, the cells were washed with 15 ml of RPMI-1640 three times. Live or fixed (with 4% paraformaldehyde) cells were observed and photographed using differential interference contrast (DIC) and GFP filters with a 40× objective on a Zeiss Axiovert microscope.

Anti-iC3b antibody (Quidel) was used to visualize iC3b associated with THP-1 cells. The cells were prepared on a coverslip (18 × 18 mm) in RPMI-1640 with 50 ng/ml PMA for 2–3 days to a density of ~0.5 × 10^5–1 × 10^5 cells/cm^2, then washed with pre-warmed serum-free RPMI-1640 five times. One hundred fifty microliters of protein-aptamer mixture was added to the cells, followed by incubation for 30 min in a humid chamber at 37°C and repeated washing in 1× PBS. Fixed cells were washed and permeabilized with 150 μl of 0.2% Triton X-100 in 1× PBS for 5 min, followed by successive incubation with anti-iC3b antibody and Alexa Fluor 594 secondary antibody (Molecular Probes) for an hour each before photography. To visualize lysosomes in live cells, 25 nM (final concentration) LysoTracker red DND99 (Invitrogen) was

added to the cell suspension during endocytosis. For bi-color detection of GFP-mCherry fusion protein, GFP and rhodamine filters were used (14).

RESULTS

Isolation of RNA aptamers for C3 and its derivatives

Because the aptamer that recognizes C3b/iC3b serves as the 'utility' moiety of the bi-functional adaptor molecule, this aptamer must not interfere with the function of C3b/iC3b; otherwise the receptors on the effector cells might be prevented from recognizing the complex. Aptamers are selected according to their ability to bind to any site on a molecule (7,8). However, review of a large number of aptamers revealed a tendency for aptamers to 'home' to active sites on the surface of a protein and inhibit the activity of their targets (15,16). To avoid isolating inhibitory aptamers for C3b/iC3b, we adopted an indirect strategy making use of the process of C3 activation. Native C3 is a complex and flexible protein, which is biologically inactive (17). Proteolytic cleavage of C3 causes a dramatic conformational change and yields its active form, C3b (2–4). The prominent structural differences between C3 and C3b result from this conformational rearrangement. In addition to the activated form of the thioester, many other binding sites are exposed through this conversion. Subsequent proteolytic products such as iC3b and C3c retain the major structural features of C3b (5). Therefore, an aptamer capable of recognizing either C3 or C3b/iC3b is unlikely to bind to the active sites revealed only following proteolytic activation.

Based on this reasoning, we selected RNA aptamers for C3 and tested their binding to C3b/iC3b. Using C3 as the target, we performed seven rounds of selection and amplification, and sequenced 54 individual clones in the final pool. We found that the most abundant sequence (Figure 1A) occurred nine times, and the second most abundant sequence occurred seven times. Both sequences demonstrated specific binding to C3 and were named AptC3-1 and AptC3-2, respectively. As shown in Figure 1B, their dissociation constants as measured by filter binding were ~18 nM for AptC3-1 and ~20 nM for AptC3-2. The RNA–protein complexes formed by these two aptamers showed different mobility in an EMSA (Figure 1C), indicating that they probably bind the C3 protein at different sites (18). (This is also supported by a competition assay presented in Supplementary Data.) We subsequently tested the affinity of both aptamers to C3b and iC3b. As shown in Figure 1C, while AptC3-1 can bind both C3b and iC3b with similar affinity, AptC3-2 showed affinity only to C3b. Because iC3b is the predominant C3-derived opsonin *in vivo* (19), we decided to use AptC3-1 as the first utility aptamer in the bi-functional construct. For this purpose, we mapped the regions necessary for its function using deletions and mutations, and identified a smaller portable structure as shown in Figure 1A (see Supplementary Data for details). We also performed a hemolytic assay and confirmed that AptC3-1 did not inhibit general complement function.
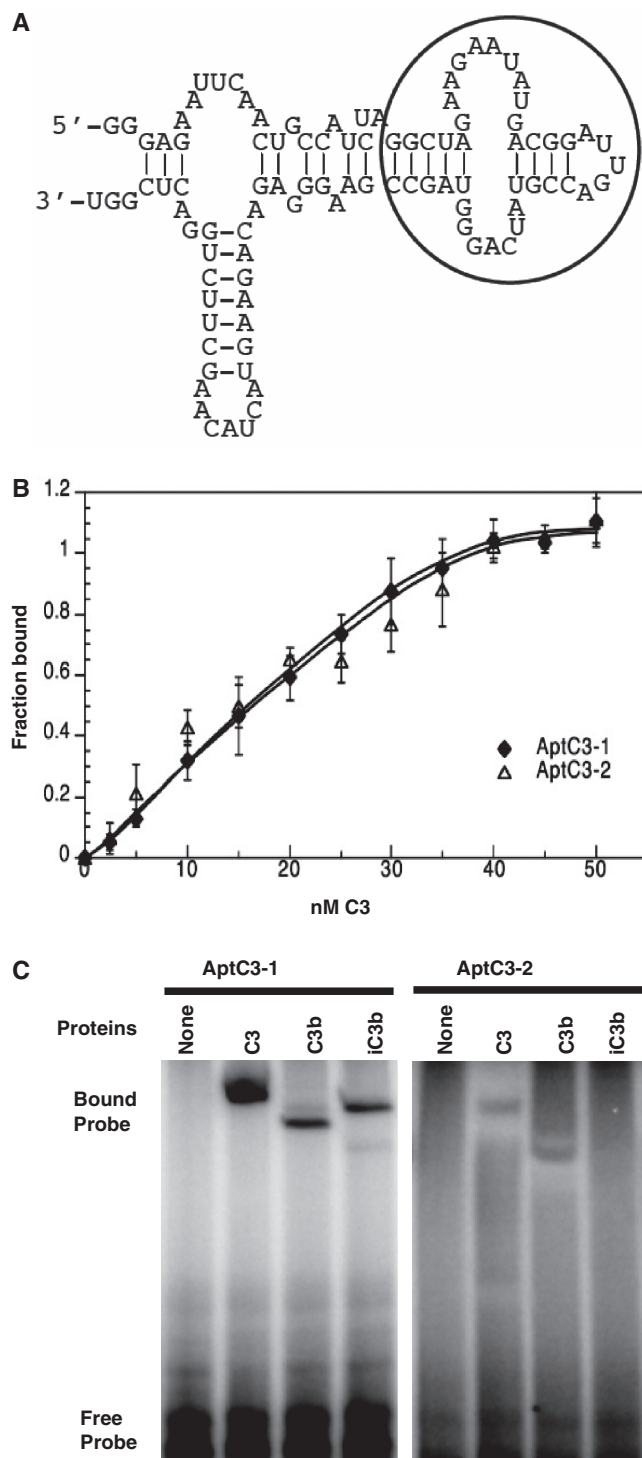

Figure 1. RNA aptamers for C3 and its derivatives. (**A**) Secondary structure of full length AptC3-1 with its minimized version encircled. This structure was predicted using the *mfold* program (48) and supported by mutational analyses. (**B**) Affinity of AptC3-1 and AptC3-2 for C3 as measured by filter binding. Values represent the average of three independent assays. Error bars indicate standard deviations. (**C**) EMSA results for AptC3-1 and AptC3-2 binding to C3, C3b or iC3b.

Construction of a bi-functional aptamer and demonstration of triple-complex formation

The simplest version of a bi-functional aptameric adaptor is composed of one targeting aptamer and one utility aptamer. We chose the GFP as a surrogate target molecule because its fluorescent signal can be conveniently followed by visual inspection in a functional assay to demonstrate the proposed mechanism. Previously, we had developed RNA aptamers that functionally interact with GFP (20), including AptGFP-AP3, which binds GFP with a K_d of 14.4 nM. To construct our first bi-functional aptamer, we joined the minimized version of AptC3-1 with AptGFP-AP3 to form the dimeric construct Apt[C3-GFP] depicted in Figure 2A. We then demonstrated that both aptamers are functional in the composite. As shown in Figure 2B, this RNA molecule possessed the ability to bind GFP and C3b or iC3b. In addition, Apt[C3-GFP] interacted with the GFP derivative d2EGFP, but not with Azami Green or mCherry, fluorescent proteins unrelated to GFP (21) (Figure 2B).

For the bi-functional aptamer to act as a molecular adaptor, it must bind both ligands independently and simultaneously. In the assay outlined in Figure 2C, we examined the capability of C3b/iC3b, Apt[C3-GFP] and GFP to form a stable triple complex. We first immobilized C3 or its derivatives on a nitrocellulose membrane and blocked the membrane with an excess of BSA. Then Apt[C3-GFP] and GFP were added sequentially to the membrane. The membrane was washed extensively after

each incubation. Membrane-bound proteins were extracted and probed with anti-GFP antibody in western blot analysis. As shown in Figure 2D, GFP was detected only when the bi-functional aptamer was present, indicating that the aptameric adaptor was indeed able to connect the two proteins.

Specific association of GFP with macrophages mediated by the bi-functional aptamer and iC3b

We developed a cell-based functional assay to examine whether the bi-functional aptamer could promote specific association of GFP with macrophages in the presence of iC3b. Analogous to the clearance of immune complexes, this experimental system is composed of four purified components: phagocytic cells, C3b or iC3b molecules, Apt[C3-GFP] and GFP or its derivatives. To represent phagocytes, we chose the human acute monocytic leukemia cell line THP-1 (22). This cell line expresses Fc and C3b receptors, but lacks surface and cytoplasmic immunoglobulins. Treatment with phorbol esters can induce THP-1 cells to differentiate into macrophage-like cells that adhere to tissue-culture surfaces (23). Before using this cell line in our assays, we confirmed the expression of CR3, the predominant iC3b receptor, by immunostaining.

Because phagocytes have a natural tendency to engulf substances added to the medium, we designed two types of controls to demonstrate the specificity of aptamer-mediated phagocytosis. In the first type, one molecular
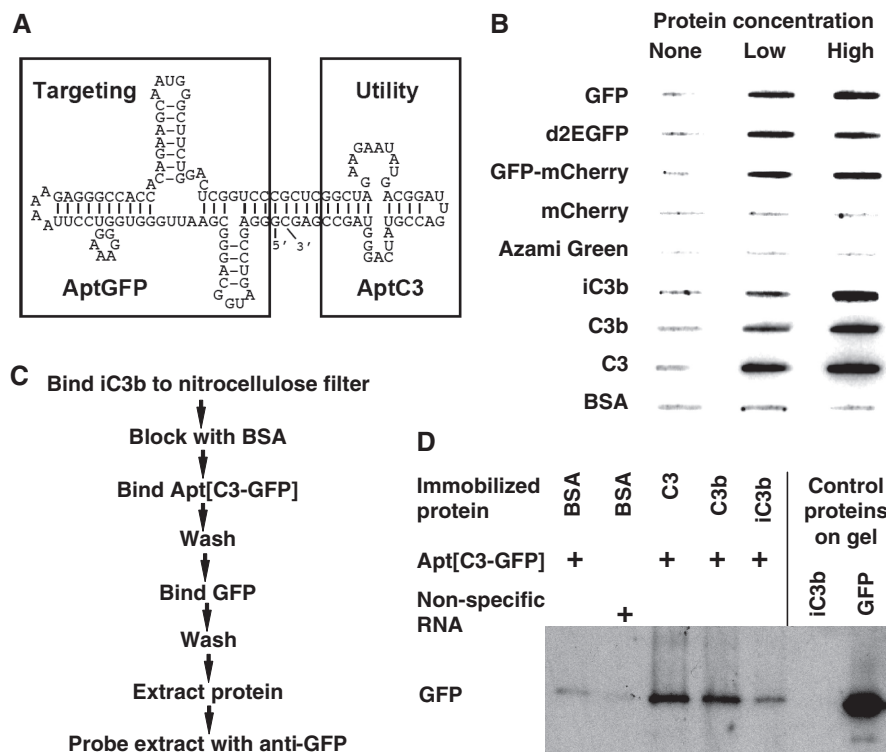

Figure 2. Bi-functional aptamer and formation of the triple complex. (**A**) Predicted secondary structure of Apt[C3-GFP]. Individual aptamers in the composite molecule are enclosed in boxes. (**B**) Binding of Apt[C3-GFP] to C3 (or its derivatives) or GFP (or its derivatives). The 'low' and 'high' concentrations are 50 and 250 nM for the fluorescent proteins, C3b and iC3b; 20 and 100 nM for C3; and 500 nM and 1 μM for BSA. (**C**) Schematic diagram of the protocol used to demonstrate triple complex formation. (**D**) Detection of triple complex formation.

Experimental (GFP + Apt[C3-GFP] + iC3b)

Control (GFP + Apt[C3-GFP])

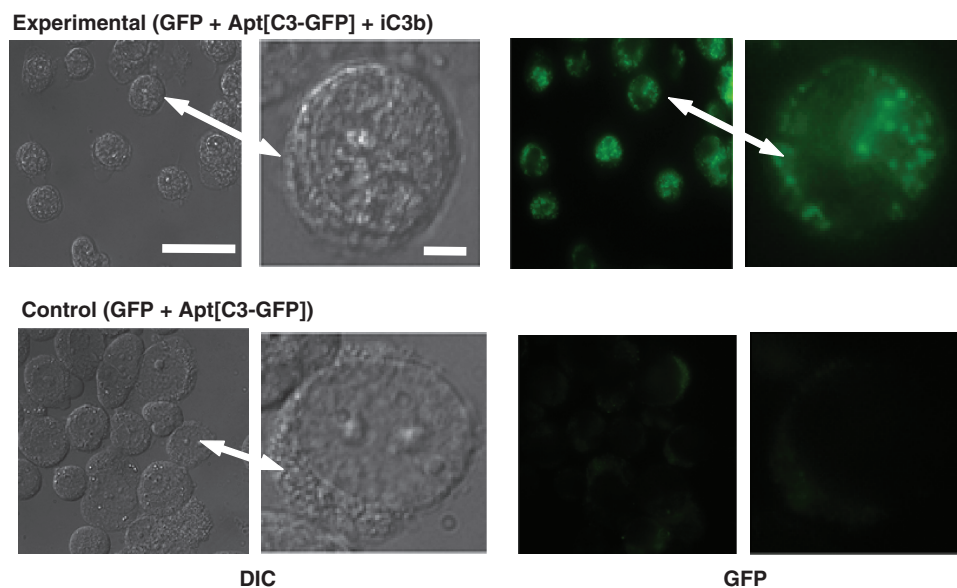DIC   GFP

Figure 3. Aptamer-dependent GFP association with unfixed THP-1 cells. Representative micrographs of cells at two different magnifications, using differential interference contrast (DIC) or a green fluorescence filter. Scale bars indicate 50 and 5 μm, respectively. In the experimental panel, cells were incubated with Apt[C3-GFP], GFP and iC3b. iC3b was omitted in the control. Cells were washed with ice-cold serum-free RPMI medium and kept on ice before photography.

component (C3b/iC3b, Apt[C3-GFP], or GFP) was omitted. In the second type, GFP was replaced with a fluorescent protein not recognized by AptGFP-AP3. In these assays the THP-1 cells were maintained as a continuous culture grown in suspension. The cells were incubated with iC3b, Apt[C3-GFP] and GFP or its derivatives (or combinations of two of these three components as controls) for 15–30 min. Live cells were washed extensively, and then examined under a microscope. Figure 3 presents fluorescent microscope images of non-adherent THP-1 cells at two different magnifications to show representative numbers of GFP-labeled cells and details of a single cell. In the experimental panels, cells treated with GFP, iC3b and Apt[C3-GFP] showed a strong signal for GFP, which was localized in vesicles, in more than 90% of the cell population. The control panels showed that in the absence of iC3b, only a weak and diffuse signal was detectable in cells. Neither Azami Green or mCherry produced fluorescent signals in THP-1 cells when these proteins were substituted for GFP. Together these controls confirmed that both the aptamer and the opsonin iC3b were necessary to generate the green fluorescent signal.

Aptamer-initiated transportation of extracellular GFP to lysosomes

Next, we verified that the opsonization-phagocytosis pathway was commandeered by the bi-functional aptamer. To demonstrate that the triple complex (iC3b, Apt[C3-GFP] and GFP) was responsible for the specific uptake of GFP by the phagocytes, we used anti-iC3b antibody to localize and visualize iC3b molecules associated with the THP-1 cells. If the bi-functional aptamer acted as a molecular adaptor, then GFP and iC3b should co-localize. Indeed, as shown in Figure 4A,

when the images with GFP signals and anti-iC3b signals were merged, we observed perfect co-localization of the two. To improve the quality of images for overlay in this experiment, we used fixed and permeabilized adherent THP-1 cells that had been stimulated to differentiate by 50 ng/ml phorbol myristate acetate. As mentioned before, these differentiated cells mimic native monocyte-derived macrophages in several aspects (12,13).

Particles are internalized by cells by means of two primary mechanisms. Small particles (<0.5 μm in diameter) such as macromolecules and viruses enter cells through receptor-mediated endocytosis, which is a clathrin-based mechanism. Large particles (>0.5 μm) are taken up into cells by actin-dependent phagocytosis (1). C3b receptors are involved in both types of internalization (24,25). Whereas the starting point of this pathway is the cell surface receptor that recognizes the opsonin, the end point is the lysosome. We noticed that after incubation of the cells with iC3b, Apt[C3-GFP] and GFP, green fluorescence was concentrated in endosome-like vesicles. To investigate the identity of these structures, we visualized GFP using the same experimental setup described above, and used LysoTracker, an acidophilic dye, to visualize lysosomes. As shown in Figure 4B, the merged image showed distinct co-localization of GFP with lysosomes. Although a low background level of GFP might occur as a result of nonspecific endocytosis, here GFP is strongly and specifically detectable in the lysosomes, suggesting that we have successfully commandeered the intended pathway.

Degradation of target molecules in the lysosome

The major objective of commandeering the opsonization-phagocytosis pathway is down-regulation of target proteins. However, GFP is a poor subject for investigation
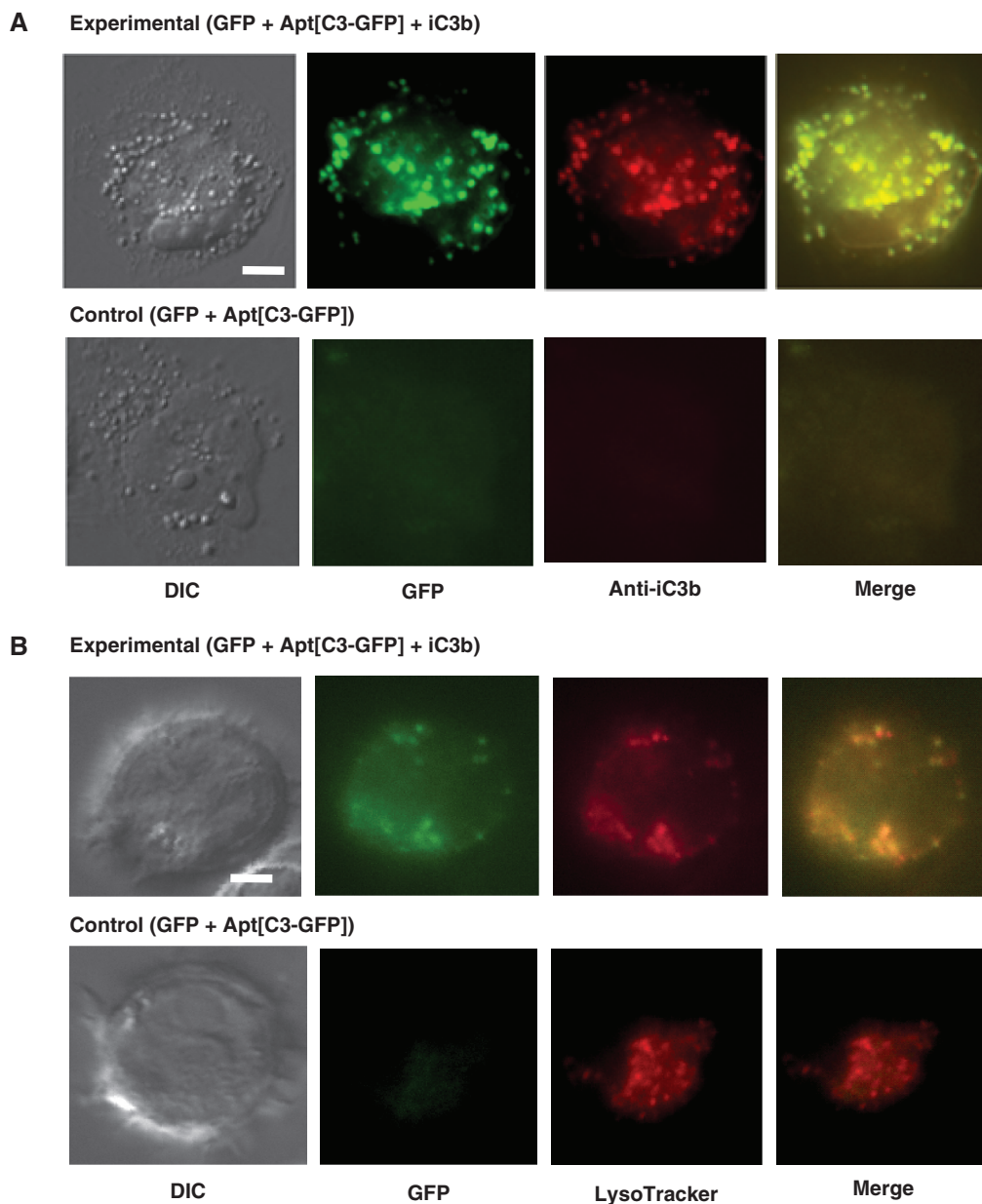
A **Experimental (GFP + Apt[C3-GFP] + iC3b)**

Control (GFP + Apt[C3-GFP])

| DIC | GFP | Anti-iC3b | Merge |

B **Experimental (GFP + Apt[C3-GFP] + iC3b)**

Control (GFP + Apt[C3-GFP])

| DIC | GFP | LysoTracker | Merge |

Figure 4. Clearance of opsonized particles by the commandeered pathway. (**A**) Co-localization of GFP with iC3b molecules. iC3b molecules were visualized using anti-iC3b antibodies. The experimental panel shows cells that were incubated with Apt[C3-GFP], GFP and iC3b. iC3b was omitted in the control. (**B**) Co-localization of GFP with lysosomes. Lysosomes were visualized using the LysoTracker dye. The cells in the experimental panel were incubated with Apt[C3-GFP], GFP, iC3b and Lysotracker. iC3b was omitted in the control. Cells were fixed with 4% paraformaldehyde. Scale bars in both panels indicate 5 μm.

of the ultimate fate of generic target proteins after reaching lysosomes, because the green fluorescent signals would be expected to persist for several days in THP-1 cells due to the extraordinary stability of GFP (26–28). After successfully tracking the path traveled by GFP even in the harsh environment of lysosomes, we addressed this issue by employing two GFP derivatives that are modified to degrade in a manner more like that of most other proteins.

First, we used d2EGFP, a destabilized variant of the enhanced GFP (eGFP) with residues 422–461 of mouse ornithine decarboxylase (MODC) fused to its C-terminus (29). This region of the MODC contains a PEST amino acid sequence that causes rapid protein turnover (30), and the degradation of d2EGFP correlates with decay of its fluorescent signal (29). As shown in Figure 2B, AptGFP-AP3 included in our construct bound d2EGFP with an affinity similar to that for GFP. In solution, the fluorescence of d2EGFP is comparable to that of GFP in the presence or absence of aptamer binding. However, when d2EGFP was used in our cell-based assay, the fluorescent signal was barely visible after incubation, suggesting that the protein has a very short half-life after uptake by the cells (Figure 5A).
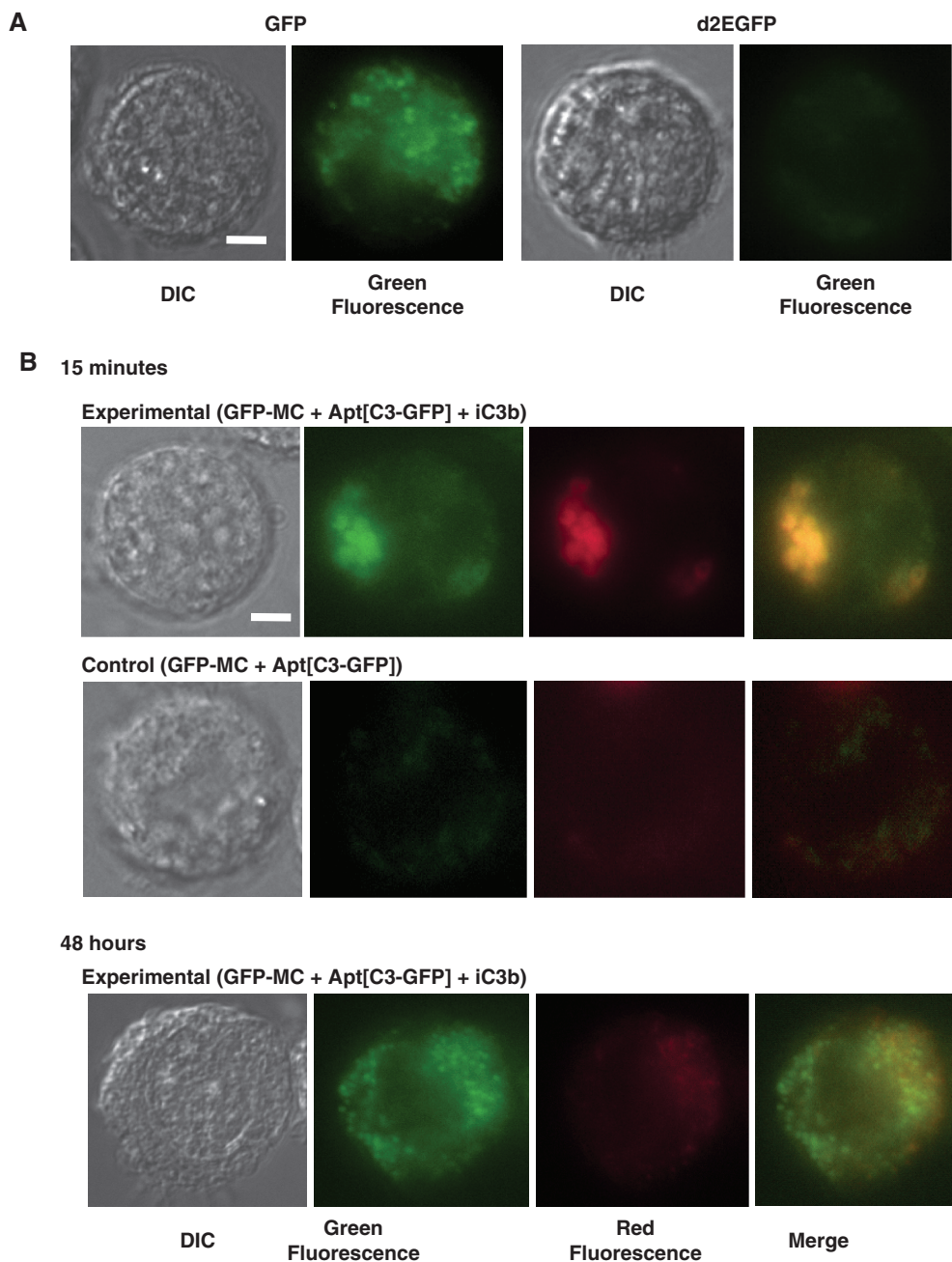
A

Figure 5. Destruction of target molecules in lysosomes. (**A**) Rapid disappearance of the d2EGFP signal compared to that of GFP. The THP-1 cells were incubated with Apt[C3-GFP], iC3b and either GFP or d2EGFP. Live cells were photographed as in Figure 3. (**B**) Bi-color tracking of GFP-mCherry fusion protein. An early (15 min) and a late (48 h) stage are shown. Cells in the experimental panel were incubated with Apt[C3-GFP], GFP-mCherry (GFP-MC) and iC3b. iC3b was omitted in the control. Scale bars in both panels indicate 5 μm.

Second, to corroborate the results obtained with d2EGFP, we tested another GFP derivative, a GFP-mCherry fusion protein. In this construct, GFP is recognized by the aptamer but mCherry is not (Figure 2B). The two fluorescent proteins are connected via a peptide linker and function independently. The dual green and red fluorescent signals of GFP-mCherry afforded a much more specific test than d2EGFP, whose signals quickly disappeared when used as the target for Apt[C3-GFP]. As shown in Figure 5B, as time elapsed a gradual dissociation of the two types of fluorescent signals was observed. Compared to the green signals, the red signals from mCherry became more diffuse and weaker, indicating that either the peptide linker had been severed or that mCherry was degraded faster than GFP.

DISCUSSION

The idea of conscripting the complement system for cancer immunotherapy was proposed more than 20 years ago (31). Complement has a number of advantages over other systems in that it is composed of

molecules that can easily penetrate the tumor mass, and many of these molecules can be supplied locally by nearby cells (32,33). Human C3 is the most abundant complement protein in serum (1.2 mg/ml), and low levels of C3b/iC3b are constitutively available as part of the alternative pathway of complement activation involved in innate immune responses (34). At any given time, ∼0.5% of the total C3 present in fresh human plasma is in its hydrolyzed form (6). Normally, opsonization facilitates removal of antigens from the circulation by macrophages in the liver and spleen, and by monocytes and neutrophils in other tissues (35). C3b is preferentially cleared by the complement receptor CR1, and iC3b by CR3 (19). Enhancement of the immune response to targeted proteins via linkage to C3b has been demonstrated previously (36–38). On the other hand, aptamers have been widely used in diagnostic and therapeutic applications (39,40). RNA constructs containing more than one functional domain (41) and bi-functional aptamers (42) have also been reported. Therefore, polyvalent aptamers with high affinity to both a target and C3b/iC3b could promote clearance of the target by either CR1 or CR3. If the target is on the surface of a cancer cell, aptameric adaptors could increase the deposition of C3b/iC3b on the cell and promote adhesion of effector cells such as macrophages and NK cells through complement receptors, whereby cytotoxicity may ensue with the help of additional signals (43–45).

In vivo implementation of the principle proved here would require several modifications to our prototype aptameric adaptor, among which two are most important. First, our current bi-functional aptamers are natural RNA molecules. Without chemical modification they are labile in the extracellular environment. Second, as a shortcut, we used C3 as the target to select aptamers that would not be inhibitory to C3b/iC3b activity; however, aptamers to be used *in vivo* should bind only opsonins, i.e. C3b and/or iC3b, but not C3. Otherwise, C3 might 'soak up' these aptamers. We plan to address these and other issues in the next stage of development. In particular, we will perform additional *in vitro* selection experiments to identify aptamers in the form of modified RNA, such as 2′fluoro-pyrimidine RNA. This type of aptamer is more stable *in vivo*, with a half-life up to 80 h in serum (46). We have previously demonstrated that aptamers can be isolated for discrete sites on a protein (18). When aptamers recognizing different areas of the C3b/iC3b surface are isolated, some of them may not interfere with any known activity of these molecules and would be ideal for our purpose. A one-time optimization of the aptamer-C3b/iC3b interface will generate a generic utility moiety, which can be connected with any targeting aptamer using a general method we developed (47) to form diverse and specific opsonizing adaptors.

SUPPLEMENTARY DATA

Supplementary Data are available at NAR Online.

REFERENCES

1. Aderem,A. and Underhill,D.M. (1999) Mechanisms of phagocytosis in macrophages. *Annu. Rev. Immunol.*, **17**, 593–623.
2. Janssen,B.J., Christodoulidou,A., McCarthy,A., Lambris,J.D. and Gros,P. (2006) Structure of C3b reveals conformational changes that underlie complement activity. *Nature*, **444**, 213–216.
3. Wiesmann,C., Katschke,K.J., Yin,J., Helmy,K.Y., Steffek,M., Fairbrother,W.J., McCallum,S.A., Embuscado,L., DeForge,L., Hass,P.E. *et al.* (2006) Structure of C3b in complex with CRIg gives insights into regulation of complement activation. *Nature*, **444**, 217–220.
4. Abdul Ajees,A., Gunasekaran,K., Volanakis,J.E., Narayana,S.V., Kotwal,G.J. and Murthy,H.M. (2006) The structure of complement C3b provides insights into complement activation and regulation. *Nature*, **444**, 221–225.
5. Nishida,N., Walz,T. and Springer,T.A. (2006) Structural transitions of complement component C3 and its activation products. *Proc. Natl Acad. Sci. USA*, **103**, 19737–19742.
6. Sahu,A. and Lambris,J.D. (2001) Structure and biology of complement protein C3, a connecting link between innate and acquired immunity. *Immunol. Rev.*, **180**, 35–48.
7. Tuerk,C. and Gold,L. (1990) Systematic evolution of ligands by exponential enrichment: RNA ligands to bacteriophage T4 DNA polymerase. *Science*, **249**, 505–510.
8. Ellington,A.D. and Szostak,J.W. (1990) In vitro selection of RNA molecules that bind specific ligands. *Nature*, **346**, 818–822.
9. Dollins,C.M., Nair,S. and Sullenger,B.A. (2008) Aptamers in immunotherapy. *Human Gene Therapy*, **19**, 443–450.
10. Shi,H., Hoffman,B.E. and Lis,J.T. (1997) A specific RNA hairpin loop structure binds the RNA recognition motifs of the Drosophila SR protein B52. *Mol. Cell. Biol.*, **17**, 1649–1657.
11. Fan,X., Shi,H., Adelman,K. and Lis,J.T. (2004) Probing TBP interactions in transcription initiation and reinitiation with RNA aptamers that act in distinct modes. *Proc. Natl Acad. Sci. USA*, **101**, 6934–6939.
12. Kohro,T., Tanaka,T., Murakami,T., Wada,Y., Aburatani,H., Hamakubo,T. and Kodama,T. (2004) A comparison of differences in the gene expression profiles of phorbol 12-myristate 13-acetate differentiated THP-1 cells and human monocyte-derived macrophage. *J. Atheroscler. Thromb.*, **11**, 88–97.
13. Whatling,C., Bjork,H., Gredmark,S., Hamsten,A. and Eriksson,P. (2004) Effect of macrophage differentiation and exposure to mildly oxidized LDL on the proteolytic repertoire of THP-1 monocytes. *J. Lipid Res.*, **45**, 1768–1776.
14. Anderson,K.I., Sanderson,J., Gerwig,S. and Peychl,J. (2006) A new configuration of the Zeiss LSM 510 for simultaneous optical separation of green and red fluorescent protein pairs. *Cytometry A*, **69**, 920–929.
15. Gold,L., Polisky,B., Uhlenbeck,O. and Yarus,M. (1995) Diversity of oligonucleotide functions. *Annu. Rev. Biochem.*, **64**, 763–797.

16. Wilson,D.S. and Szostak,J.W. (1999) In vitro selection of functional nucleic acids. *Annu. Rev. Biochem.*, **68**, 611–647.

17. Janssen,B.J., Huizinga,E.G., Raaijmakers,H.C., Roos,A., Daha,M.R., Nilsson-Ekdahl,K., Nilsson,B. and Gros,P. (2005) Structures of complement component C3 provide insights into the function and evolution of immunity. *Nature*, **437**, 505–511.

18. Shi,H., Fan,X., Sevilimedu,A. and Lis,J.T. (2007) RNA aptamers directed to discrete functional sites on a single protein structural domain. *Proc. Natl Acad. Sci. USA*, **104**, 3742–3746.

19. Yan,J., Vetvicka,V., Xia,Y., Hanikyrova,M., Mayadas,T.N. and Ross,G.D. (2000) Critical role of Kupffer cell CR3 (CD11b/CD18) in the clearance of IgM-opsonized erythrocytes or soluble beta-glucan. *Immunopharmacology*, **46**, 39–54.

20. Kotlikoff,M., Shi,H., Shui,B. and Lis,J.T. (2009) Functional nucleic acid ligands to fluorescent proteins, *US Patent Application Publication No*. US 2009/0197271 A1.

21. Shaner,N.C., Campbell,R.E., Steinbach,P.A., Giepmans,B.N., Palmer,A.E. and Tsien,R.Y. (2004) Improved monomeric red, orange and yellow fluorescent proteins derived from Discosoma sp. red fluorescent protein. *Nat. Biotechnol.*, **22**, 1567–1572.

22. Tsuchiya,S., Yamabe,M., Yamaguchi,Y., Kobayashi,Y., Konno,T. and Tada,K. (1980) Establishment and characterization of a human acute monocytic leukemia cell line (THP-1). *Int. J. Cancer*, **26**, 171–176.

23. Tsuchiya,S., Kobayashi,Y., Goto,Y., Okumura,H., Nakae,S., Konno,T. and Tada,K. (1982) Induction of maturation in cultured human monocytic leukemia cells by a phorbol diester. *Cancer Res.*, **42**, 1530–1536.

24. Fearon,D.T., Kaneko,I. and Thomson,G.G. (1981) Membrane distribution and adsorptive endocytosis by C3b receptors on human polymorphonuclear leukocytes. *J. Exp. Med.*, **153**, 1615–1628.

25. Abrahamson,D.R. and Fearon,D.T. (1983) Endocytosis of the C3b receptor of complement within coated pits in human polymorphonuclear leukocytes and monocytes. *Lab. Invest.*, **48**, 162–168.

26. Cubitt,A.B., Heim,R., Adams,S.R., Boyd,A.E., Gross,L.A. and Tsien,R.Y. (1995) Understanding, improving and using green fluorescent proteins. *Trends Biochem. Sci.*, **20**, 448–455.

27. Ormo,M., Cubitt,A.B., Kallio,K., Gross,L.A., Tsien,R.Y. and Remington,S.J. (1996) Crystal structure of the Aequorea victoria green fluorescent protein. *Science*, **273**, 1392–1395.

28. Yang,F., Moss,L.G. and Phillips,G.N. Jr (1996) The molecular structure of green fluorescent protein. *Nat. Biotechnol.*, **14**, 1246–1251.

29. Li,X., Zhao,X., Fang,Y., Jiang,X., Duong,T., Fan,C., Huang,C.C. and Kain,S.R. (1998) Generation of destabilized green fluorescent protein as a transcription reporter. *J. Biol. Chem.*, **273**, 34970–34975.

30. Rechsteiner,M. and Rogers,S.W. (1996) PEST sequences and regulation by proteolysis. *Trends Biochem. Sci.*, **21**, 267–271.

31. Cooper,P.D. (1985) Complement and cancer: activation of the alternative pathway as a theoretical base for immunotherapy. *Adv. Immun. Cancer Ther.*, **1**, 125–166.

32. Gelderman,K.A., Tomlinson,S., Ross,G.D. and Gorter,A. (2004) Complement function in mAb-mediated cancer immunotherapy. *Trends Immunol.*, **25**, 158–164.

33. Macor,P. and Tedesco,F. (2007) Complement as effector system in cancer immunotherapy. *Immunol. Lett.*, **111**, 6–13.

34. Carroll,M.C. (1998) The role of complement and complement receptors in induction and regulation of immunity. *Annu. Rev. Immunol.*, **16**, 545–568.

35. Tosi,M.F. (2005) Innate immune responses to infection. *J. Allergy Clin. Immunol.*, **116**, 241–249; quiz 250.

36. Villiers,M.B., Villiers,C.L., Jacquier-Sarlin,M.R., Gabert,F.M., Journet,A.M. and Colomb,M.G. (1996) Covalent binding of C3b to tetanus toxin: influence on uptake/internalization of antigen by antigen-specific and non-specific B cells. *Immunology*, **89**, 348–355.

37. Villiers,M.B., Villiers,C.L., Laharie,A.M. and Marche,P.N. (1999) Amplification of the antibody response by C3b complexed to antigen through an ester link. *J. Immunol.*, **162**, 3647–3652.

38. Villiers,M.B., Marche,P.N. and Villiers,C.L. (2003) Improvement of long-lasting response and antibody affinity by the complexation of antigen with complement C3b. *Int. Immunol.*, **15**, 91–95.

39. Drolet,D.W., Nelson,J., Tucker,C.E., Zack,P.M., Nixon,K., Bolin,R., Judkins,M.B., Farmer,J.A., Wolf,J.L., Gill,S.C. *et al.* (2000) Pharmacokinetics and safety of an anti-vascular endothelial growth factor aptamer (NX1838) following injection into the vitreous humor of rhesus monkeys. *Pharm. Res.*, **17**, 1503–1510.

40. Golden,M.C., Collins,B.D., Willis,M.C. and Koch,T.H. (2000) Diagnostic potential of PhotoSELEX-evolved ssDNA aptamers. *J. Biotechnol.*, **81**, 167–178.

41. SenGupta,D.J., Zhang,B., Kraemer,B., Pochart,P., Fields,S. and Wickens,M. (1996) A three-hybrid system to detect RNA-protein interactions in vivo. *Proc. Natl Acad. Sci. USA*, **93**, 8496–8501.

42. Burke,D.H. and Willis,J.H. (1998) Recombination, RNA evolution, and bifunctional RNA molecules isolated through chimeric SELEX. *RNA*, **4**, 1165–1175.

43. Ross,G.D., Vetvicka,V., Yan,J., Xia,Y. and Vetvickova,J. (1999) Therapeutic intervention with complement and beta-glucan in cancer. *Immunopharmacology*, **42**, 61–74.

44. Hong,F., Hansen,R.D., Yan,J., Allendorf,D.J., Baran,J.T., Ostroff,G.R. and Ross,G.D. (2003) Beta-glucan functions as an adjuvant for monoclonal antibody immunotherapy by recruiting tumoricidal granulocytes as killer cells. *Cancer Res.*, **63**, 9023–9031.

45. Li,B., Allendorf,D.J., Hansen,R., Marroquin,J., Ding,C., Cramer,D.E. and Yan,J. (2006) Yeast beta-glucan amplifies phagocyte killing of iC3b-opsonized tumor cells via complement receptor 3-Syk-phosphatidylinositol 3-kinase pathway. *J. Immunol.*, **177**, 1661–1669.

46. Kubik,M.F., Bell,C., Fitzwater,T., Watson,S.R. and Tasset,D.M. (1997) Isolation and characterization of 2′-fluoro-, 2′-amino-, and 2′-fluoro-/amino-modified RNA ligands to human IFN-gamma that inhibit receptor binding. *J. Immunol.*, **159**, 259–267.

47. Xu,D. and Shi,H. (2009) Composite RNA aptamers as functional mimics of proteins. *Nucleic Acids Res.*, **37**, e71.

48. Zuker,M. (2003) Mfold web server for nucleic acid folding and hybridization prediction. *Nucleic Acids Res.*, **31**, 3406–3415.